-Technical Paper-

Shear Force-Relative Displacement Relationships of L-shape Shear Connector Subjected to Strut Compressive Force

Soty ROS*1 and Hiroshi SHIMA*2

ABSTRACT

This study investigates the relationships between shear force and relative displacement of L-shape shear connector by means of beam type test method. Based on experimental results, an equation to predict the ultimate shear capacity of L-shape shear connector at split failure occurrence was developed. Moreover, an equation for the enveloped curve of shear force-relative displacement relationship of the shear connector was proposed. The ultimate relative displacement was found to be approximately 0.02 times the height of the shear connector regardless of strut angle and concrete strength.

Key words: L-shape shear connector, ultimate shear capacity, ultimate relative displacement

1. INTRODUCTION

Shear connector is a structural component used to mechanically connect steel with concrete. It is generally used as the shear resistance in steel-concrete interface in steel-concrete composite structures. The performance of the shear connectors is known to have great influence on the monolithic behavior of this kind of structure. Usually, in the design, steel-concrete interaction has been considered to be fully interacted and only the shear capacity of the shear connector itself has been focused. However, the design will be more rational by taking shear force-relative displacement relationship of the shear connector into account. If the relative displacements of the shear connectors are allowed in design, it means that the shear connectors are allowed to resist higher level of shear force and the number of shear connectors can be reduced as compared to the design with fully interaction. Therefore, in the design the shear force-relative displacement relationship of the shear connector is important for designers to determine the allowable value of relative displacement corresponding to the allowable shear force of shear connector.

The formulations for shear capacity of plate shape shear connector [1], [2], shape steel shear connector [3], and angle shape shear connector [4] were previously studied and proposed by taking into account the size of the shear connector and the concrete strength. Also, the transferred shear force-relative displacement relationship of different types of shear connectors in steel-concrete sandwich beam were investigated [5], [6], [7]. Additionally, the formulations for both shear capacity and shear force-slip relationship's curve of headed stud, block dowel, and perforated-bond plate shear connectors have already been proposed by JSCE standard specifications for hybrid structures [8]. However, those of L-shape shear connector have not yet been confirmed.

Fortunately, the study of the behavior of L-shape shear connector subjected to strut compressive force was recently conducted by means of beam type test method [9], [10], [11]. Based on experimental results and FEM analyses, the formulations for ultimate shear force at split failure and for shear force-relative displacement relationship's curve were developed. However, the equations were proposed only in case that strut angle was equal to 45°. Therefore, this study aimed to clarify the applicable range of the previous equations [11] by integrating the experimental results of one more specimen whose strut angle smaller than 45°.

2. EXPERIMENT

The specimens are symbolized as S-height of specimen-height of shear connector-thickness of shear connector-concrete strength-strut angle (S-h-h_{sc}-t_{sc}-f_c'-θ). S-300-100-9-41.5-25 is an additional specimen whose concrete strength was 41.5 N/mm^2 and strut angle was 25°. Fig.1 and Table 1 give the details all specimens including the shear connector and the support. A flexural crack initiator with section ($b \times h_c$) was inserted at mid span of the new specimen, Fig.1a). Since the specimen failed very late after flexural crack occurrence, the flexural crack initiator did not affect the behavior of the shear connector. JIS G 3101 standard steel with grade SM490 and grade SS400 whose properties are given in Table 2 was used for the steel plate and the shear connector, respectively.

The same measurements were made for all specimens. Strain distributions in the skin plate in front of the shear connector were measured by strain gauges of 5mm length, R1 to R4, Fig.2. Moreover, the concrete-skin plate slip and the relative displacement of the shear connector were measured by the displacement transducers whose locations are illustrated in Fig.3 and Fig.4, respectively. The average values obtained from the

*1 Phd Student, Dept. of Infrastructure System Engineering, Kochi University of Technology, JCI Member
*2 Professor, Dept. of Infrastructure System Engineering Kochi University of Technology, JCI Member

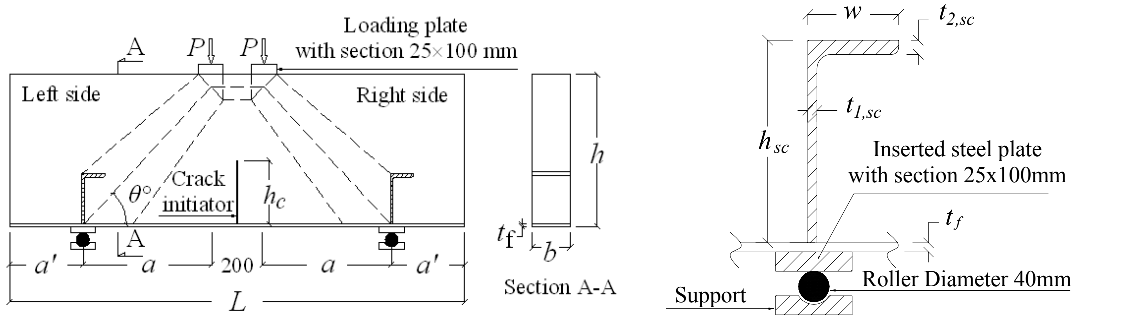

a) Details of specimens b) Details of shear connector and support

Fig. 1 Details of specimens and support

Table 1 Details of all specimens

Specimens	Sizes of Specimens (mm)							Sizes of shear connectors (mm)				Thick-ness of skin plate t_f (mm)	Concrete strength f_c' (N/mm^2)
	a	b	h	L	a'	θ	h_c	h_{sc}	w	$t_{1,sc}$	$t_{2,sc}$		
S-600-200-9-38-45	510	150	600	1800	300	45	-	200	90	9	14	9	38.0
S-600-200-9-25-45	510	150	600	1800	300	45	-	200	90	9	14	9	25.3
S-450-150-9-24-45	410	150	450	1500	250	45	-	150	75	9	14	9	23.6
S-300-100-9-25-45	290	150	300	1100	200	45	-	100	50	9	14	9	25.1
S-300-100-9-41.5-25	500	150	300	1600	200	25	150	100	50	9	14	9	41.5

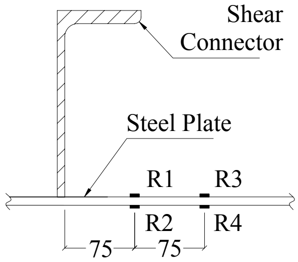

Fig. 2 Strain gauges locations

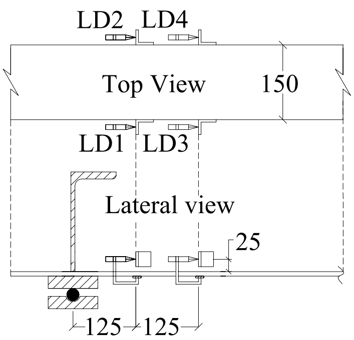

Fig. 3 Slip measurement

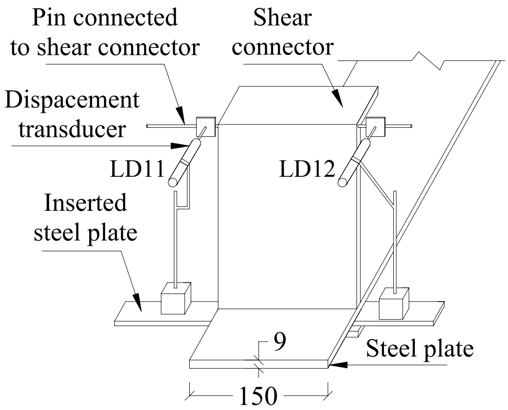

Fig. 4 Relative displacement measurement

Table 2 Characteristics of steel

	Shear Connector	Skin Plate
Tensile yield strength f_y (N/mm^2)	352	370
Ultimate strength f_u (N/mm^2)	448	511
Modulus of elasticity E (kN/mm^2)	202	204

displacement transducers LD1 to LD4 were determined as the slip and those obtained from LD11 and LD12 were determined as the relative displacement the shear connector.

3. RESULTS AND DISCUSSIONS

3.1 Failure mode of specimens

Since only left size shear connectors failed, the discussions are accordingly made in this study. Fig.5 gives the condition at failure and the crack pattern of S-300-100-9-41.5-25. The numbers shown in the figure represented the load 2P in kN. The specimen was found to fail at the occurrence of splitting crack in the concrete in front of the shear connector which is the same failure mode and crack pattern observed in the previous four specimens [9], [10], [11]. Moreover, similar shear resisting mechanism was observed. The shear connector was still able to resist against the shear force even though the first diagonal crack already appeared in the concrete from the head of the shear connector. This behavior proved the advantage of the test method used while shear connectors in push-out and direct pull-out test methods were found to gradually lose their shear resisting ability after the occurrences on crack from their heads [1], [2], [3], [4]. The experimental result of S-300-100-9-41.5-25 showed that split failure could also occur in case of strut angle smaller than 45^o.

The behavior of L-shape shear connector before and at split failure can be simply explained as illustrated in Fig.6. It is assumed that the shear connector was subjected strut compressive force F with strut direction θ. Before split failure, Fig.6a) the concrete in front of the shear connector seemed to resist against a multidirection

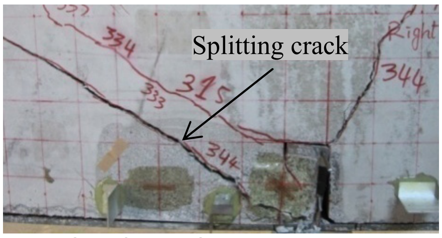

a) Split failure S-300-100-9-41.5-25

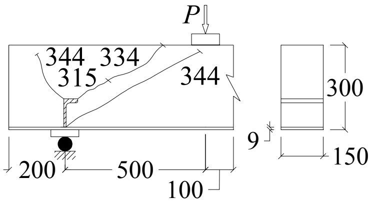

b) Crack pattern S-300-100-9-41.5-25

Fig. 5 S-300-100-9-41.5-25 at failure

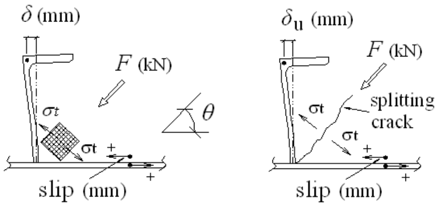

a) Before split failure b) At split failure

Fig. 6 Shear connector before and at split failure

direction stress and this stress could be released along the direction of principal tensile stress σ_t due to the relative displacement of the shear connector δ. Finally, when the relative displacement reached its ultimate value δ_u the moment at which the principal tensile stress exceeded the tensile strength of the concrete f_t, splitting crack took place along the axis of the strut compressive force and perpendicularly with the direction of the principal tensile stress, Fig.6b).

3.2 Ultimate Shear Force

Shear force V was calculated by multiplying stress σ in the steel plate in front of the shear connector by the area of the steel plate A_s $\left(A_s = t_f \cdot b\right)$. Meanwhile, the stress was calculated by means of the stress-strain relationship of the steel plate, $(\sigma_s = E_s \cdot \varepsilon_s)$ whose strain values were obtained from the strain gauges shown in Fig.2.

Table 3 gives the summary of the ultimate shear forces V_u obtained from the experimental results $V_{u.exp}$ and the calculation results by means of the specifications for hybrid structures of JSCE [8] with all safety factors 1.0. Additionally, since there is only one shear connector in the shear span, the spacing of the shear connector used to calculate the shear capacity of L-shape shear connector V_{sc1} was infinite.

It can be observed that the calculated shear capacities of the shear connectors V_{sc1} were found to agree with $V_{u.exp}$ by chance in case of strut angle was 45° with $V_{u.exp}$ to V_{sc1} ratios varied from 1.02 to 1.11. Meanwhile, in case of strut angle was 25°, $V_{u.exp}$ to V_{sc1} ratio was up to 1.37. These results showed that the formula given by

Table 3 Calculation and Experimental results

Specimens	$V_{u.exp}$ (kN)	V_{sc1} (kN)	$V_{u.exp}$ / V_{sc1}	$V_{u.Eq2}$ (kN)	$V_{u.exp}$ / $V_{u.Eq2}$
S-600-200-9-38-45	266	240	1.11	256	1.03
S-600-200-9-25.3-45	200	195	1.02	207	0.96
S-450-150-9-23.6-45	182	171	1.06	182	0.98
S-300-100-9-25.1-45	170	154	1.11	169	1.00
S-300-100-9-41.5-25	272	198	1.37	218	1.25

the specifications for hybrid structures of JSCE [8] can conservatively predict the shear capacity of L-shape shear connector subjected to strut compressive force.

There are two reasons to explain why the calculated shear capacity of the shear connector V_{sc1} was different from the experimental results $V_{u.exp}$. Firstly, the formula of V_{sc1} was developed by means of direct pull-out test method [1], [2] where the shear connectors resisted against only longitudinal stress (θ = 0°); on the contrary, in this study the shear connectors were subjected to strut compressive force whose strut angle greater than zero (θ = 25° and 45°). Secondly the failure mode of the shear connectors observed in the direct pull-out test was different from that observed in this study. Therefore, a new formula to predict the ultimate shear capacity of L-shape shear connector subjected to strut compressive force is necessary.

3.3 Formulation for ultimate shear capacity of L-shape shear connector

The ultimate shear capacity V_u of L-shape shear connector subjected to strut compressive force at split failure occurrence was previously proposed by Ros and Shima [11] based on the experimental results of the four specimens whose strut angle was 45°. They assumed that the behavior of the concrete at which splitting crack occurred was similar to that of the cylinder in the split tensile strength test, Fig.7a). The equation was proposed as followings:

$$V_u = k_1 \cdot \sqrt{f_c'} \cdot b_{sc} \cdot h_{sc} \tag{2}$$

$$k_1 = 19.56\left(\frac{t_{1,sc}}{h_{sc}}\right) + 0.494 \tag{3}$$

Where, V_u: ultimate shear force at split failure (N), b_{sc}: width of shear connector (mm), h_{sc}: height of shear connector (mm), $t_{1,sc}$: thickness of shear connector (mm), and f_c': concrete compressive strength (N/mm²).

It can be seen in Table 3 that the ultimate shear forces calculated by means of Eq.2 $V_{u.Eq2}$ can precisely predict the ultimate shear forces of shear connectors only in case of strut angle $\theta = 45°$. However, this equation was found to underestimate the ultimate shear force when strut angle $\theta < 45°$, S-300-100-9-41.5-25 with $V_{u.exp}$ to $V_{u.Eq2}$ ratio was equal to 1.25.

Therefore, the revision of Eq.2 is necessary. It can be observed in the previous model of Ros and Shima [11], Fig.7a) that the strut compressive force on the shear connector was equal to $V_u\sqrt{2}$ which is equal to $(V_u/\cos 45)$. It means that cos45 was included in the equation of k_1, Eq.3. That is the reason why Eq.2 cannot

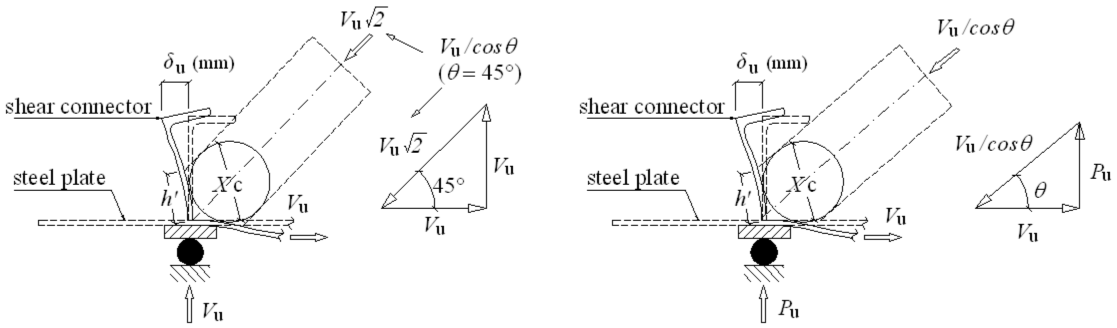

a) Previous consideration with $\theta = 45°$ a) New consideration with $\theta < 45°$

Fig.7 Model of shear connector under strut compressive force failed in split failure mode

Table 4 Calculation and Experimental results

Specimens	$V_{u.exp}$ (kN)	$V_{u.Eq4}$ (kN)	$V_{u.exp}/V_{u.Eq4}$
S-600-200-9-38-45	266	256	1.03
S-600-200-9-25.3-45	200	209	0.96
S-450-150-9-23.6-45	182	184	0.98
S-300-100-9-25.1-45	170	171	0.99
S-300-100-9-41.5-25	272	282	0.97

predict the ultimate shear forces of the shear connector when the strut angle $\theta < 45°$. Therefore, the authors decided to remove cos45 from the equation of k_1, Eq.3 and keep cosθ in Eq.2, Fig.7b). Eq.2 and Eq.3 can be replaced by Eq.4 and Eq.5, respectively.

$$V_u = k_1 \cdot \sqrt{f_c'} \cdot b_{sc} \cdot h_{sc} \cdot \cos\theta \quad (4)$$

$$k_1 = 28\left(\frac{t_{1,sc}}{h_{sc}}\right) + 0.70 \quad (5)$$

Where, V_u : ultimate shear force at split failure (N), b_{sc}: width of shear connector (mm), h_{sc}: height of shear connector (mm), $t_{1,sc}$: thickness of shear connector (mm), f_c': concrete compressive strength (N/mm^2), and θ: strut angle ($\theta > \theta_o$) (deg).

As shown in Table 4, Eq.4 can precisely predict the ultimate shear forces V_u of L-shape shear connector subjected to strut compressive force at split failure under different strut angle with $V_{u.exp}$ to $V_{u.Eq4}$ ratio varied from 0.96 to 1.03.

3.4 Shear force-slip relationships

The relationships between shear force and concrete-skin plate slip in front of the shear connector of all specimens are given in Fig.8. The experimental results showed that the stiffness of the same thickness shear connectors $(t_{1,sc} = 9\text{ mm})$ was the same despite different height of shear connector, different concrete strength and different strut angle. Moreover, since the curves of shear force-slip relationship of all shear connector were similar, no effects of concrete strength, strut angle, and size of shear connector on shear force-slip relationships' curves were observed in this study.

However, the concrete strength and strut angle were found to have effect on both the ultimate shear capacity and the ultimate slip between concrete and skin plate. It can be observed between S-600-200-9-38-45 and S-600-200-9-25.3-45 that the shear connector with

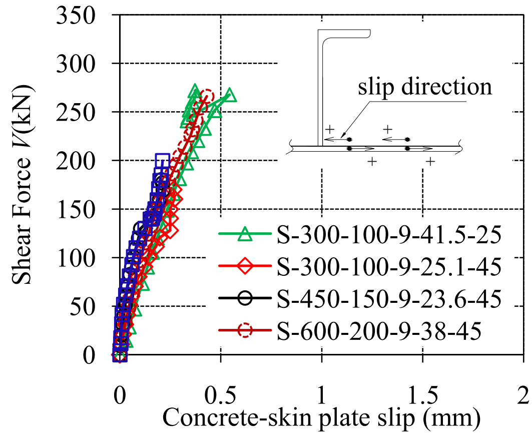

Fig. 8 Shear force-slip relationships

higher concrete strength failed at greater ultimate slip corresponding to higher level of shear force. Similarly, between S-300-100-9-25.1-45 and S-300-100-9-41.5-25 the shear connector with higher concrete strength and smaller strut angle failed at higher level of shear force corresponding to greater ultimate slip.

Additionally, it was found that concrete-skin plate slip occurred even under low load levels. Similar behaviors were also found in push-out test method and direct pull-out test method by Chuah et al. [2] and Kiyomiya et al. [3], respectively.

3.5 Shear force-relative displacement relationships

The shear force-relative displacement of the shear connector in the new specimen S-300-100-9-41.5-25 was plotted together with those of the previous two specimens [11], Fig.9.

Similarly to the previous two specimens, the shape of shear force-relative displacement relationships' curve of S-300-100-9-41.5-25 appeared after the occurrence of the first diagonal crack from the head of the shear connector. Then big increment of relative displacement with little increment of shear force was observed until the occurrence of splitting crack in the concrete in front of the shear connector. These similar behaviors were also found for L-shape shear connector in in steel-concrete sandwich beam by Saidi et al. [5], [6], [7] that the relative displacement became larger after the occurrence of crack from the head of the shear connector. However, differently from the steel concrete sandwich beam test, the ultimate relative displacements δ_u

of L-shape shear connectors subjected to strut compressive force could be obtained in the beam type test method.

Moreover, it can be observed between S-300-100-9-25.1-45 and S-300-100-9-41.5-25 whose concrete strength and strut angle were different that both specimens failed at different levels of shear force but at similar ultimate relative displacement δ_u. Therefore, it can be said that the concrete strength and the strut angle affected the ultimate shear capacity V_u of the shear connector but not the ultimate relative displacement δ_u. Similarly, the experimental results suggested that the same size shear connector gave similar ultimate relative displacement regardless of strut angle and concrete strength.

Regarding to the effect of height of the shear connector on shear force-relative displacement relationships, the different performances of the shear connector illustrated in Fig.9 can be clarified. It can be compared between S-600-200-9-25.3-45 and S-300-100-9-25.1-45 whose concrete strength and strut angle were the same that the larger size shear connector failed at greater value of ultimate relative displacement corresponding to higher level of shear force. Furthermore, even though the concrete strength of S-600-200-9-25.3-45 was lower than that of S-300-100-9-41.5-25, the ultimate relative displacement of the larger size shear connector was still greater value than that of the smaller size shear connector. Therefore, the experimental results suggested that the larger size shear connector gave greater value of ultimate relative displacement regardless of strut angle and concrete strength.

Additionally, L-shape shear connector subjected to strut compressive force in beam type specimen was found to have big increment of relative displacement with little increment of shear force after the occurrence of crack from the head of the shear connector. These results are different from those obtained from push-out test [3] and direct pull-out test specimens [4] that after crack appeared from the head of the shear connector, the relative displacement of the shear connector increased with a gradual decrease of the shear force. The different direction of stress upon the shear connector may be the reason for these differences.

Even though shear force-relative displacement relationships of L-shape shear connectors were clearly understood from the experimental results, the formula to predict the enveloped curve of the relationships also plays a vital role in the design of steel-concrete composite structures. Therefore, the following sub-chapter illustrates the formulation for the enveloped curve of shear force-relative displacement relationship of L-shape shear connector subjected to strut compressive force in steel-concrete composite structures.

3.6 Formulation for shear force-relative displacement relationships

The formula for shear force-relative displacement relationship of L-shape shear connector subjected to strut compressive force previously proposed for the case that strut angle θ approximately 45° by Ros and Shima [11]. Additionally, Eq.6 was proposed for the case after the occurrence of crack from the head of the shear connector until failure of the shear connector. The formula was expressed as followings:

$$\frac{V}{V_u} = \left(1 - e^{-180\frac{\delta}{h_{sc}}}\right)^{0.6} \tag{6}$$

Where, V_u: ultimate shear force at split failure (N), δ: relative displacement (mm), and h_{sc}: height of shear connector (mm).

The calculated results by means of Eq.6 were compared with those obtained from experiments of the additional specimen S-300-100-9-41.5-25 whose strut angle was smaller than 45° in order to examine the applicable range of the equation.

Fig.10 gives V/V_u and δ/h_{sc} relationships of the three specimens. It can be observed that when shear force V was normalized by the ultimate shear force V_u and relative displacement δ by the height of the shear connector h_{sc}, a unique enveloped curve was obtained. Moreover, the results of the calculation by means of Eq.6 agreed well with the experimental results. The normalized curve of S-300-100-9-41.5-25 whose strut angle was 25° also fitted best with the calculation results for the case after the occurrence of crack from the head of the shear connector until failure of the shear connector. These results proved the applicable range of Eq.6.

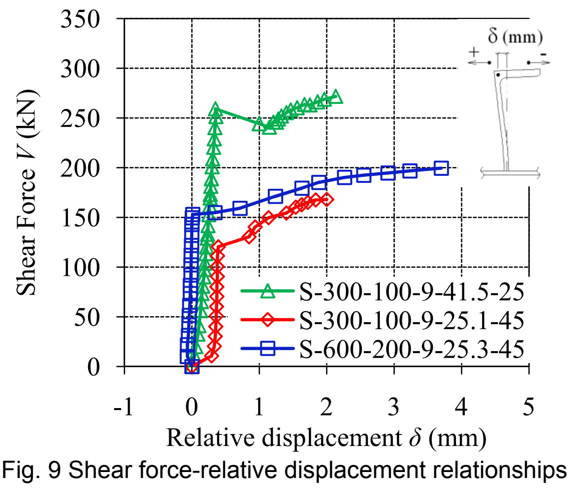

Fig. 9 Shear force-relative displacement relationships

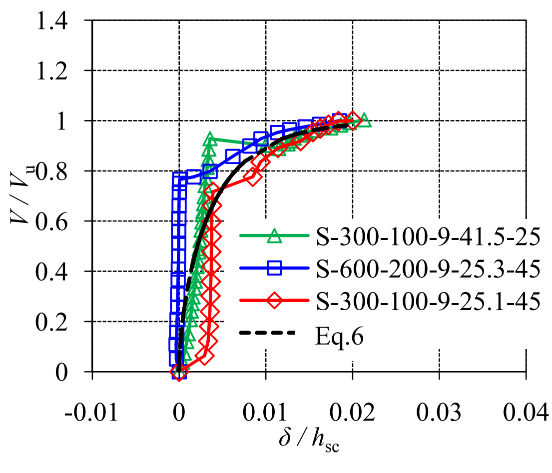

Fig. 10 V/V_u - δ/h_{sc} relationships of the shear connector

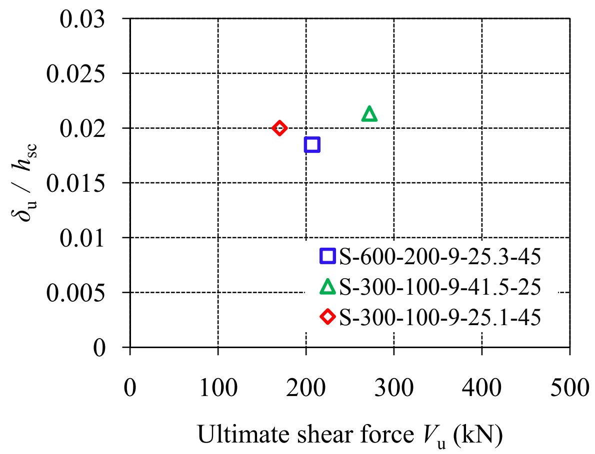

Fig. 11 V_u - δ_u/h_{sc} relationships

Therefore, it can be concluded that Eq.6 can also precisely predict the enveloped curve of shear force-relative displacement relationship of L-shape shear connector subjected to strut compressive force with strut direction smaller than 45°.

Fig.11 gives the relationships between V_u and δ_u/h_{sc} obtained from the experimental results. It can be seen that the ultimate relative displacements δ_u of the shear connectors were approximately 0.02 times the height of the shear connector regardless of the strut angle and the concrete strength.

4. CONCLUSIONS

The following conclusions can be derived from this study:

(1) Split failure mode of L-shape shear connector subjected to strut compressive force was also observed even the strut angle was smaller than 45°.

(2) The formula for ultimate shear capacity of L-shape shear connector at split failure occurrence was revised by introducing the strut angle into the equation and proposed to be:

$$V_u = k_1 \cdot \sqrt{f_c'} \cdot b_{sc} \cdot h_{sc} \cdot \cos\theta$$

$$k_1 = 28\left(\frac{t_{1,sc}}{h_{sc}}\right) + 0.70$$

(3) An equation to predict the enveloped curve of the relationships between V/V_u and δ/h_{sc} of L-shape shear connector subjected to strut compressive force regardless of the concrete strength, and strut angle is proposed as followings:

$$\frac{V}{V_u} = \left(1 - e^{-180\frac{\delta}{h_{sc}}}\right)^{0.6}$$

(4) The ultimate relative displacements δ_u of L-shape shear connectors were found approximately 0.02 times the height of the shear connector regardless of strut angle and concrete strength.

ACKNOWLEDGMENT

The authors would like to express their gratitude to members of concrete laboratory of Infrastructure System Engineering Department, Kochi University of Technology for their assistances during the experimental work.

REFERENCES

[1] Ueda, T. and Chin, C.K., "Strength of steel plate shear connector." *Proc. of the Second Symposium on Research and Application of Composite Constructions, JSCE*, 1989, pp.149-156, (in Japanese).

[2] Chuah, C.L., Shima, H., and Virach, R., "Load-displacement relationship of plate shear connector in steel-concrete composite structure." *Proc. of JSCE*, No.433/V-15, 1991, pp.223-229.

[3] Kiyomiya, O., Yokota, H., Suzuki, M., and Chiba, T., "Strength properties of shear connector by shape steel." *Transactions of the Japan Concrete Institute, JCI*, Vol. 8, 1986, pp.345-352.

[4] Yamada, M. and Kiyomiya, O., "Experimental study on the loading capacity of angle shape and headed stud shear connector for composite structures, *Transaction of The Japan Concrete Institute, JCI,* Vol. 14, 1992, pp.461-468.

[5] Saidi, T., Furuuchi, H., and Ueda, T., "Relationship between transferred shear force and relative displacement of shear connector in steel-concrete sandwich beam." *Journal of Structural Engineering, JSCE,* 44 (A), March 1998, pp.1537-1545.

[6] Saidi, T., Furuuchi, H. and Ueda, T., "Effect of shape and location of shear connector on its transferred shear force and relative displacement relationship in steel-concrete sandwich beam." *Journal of Structural Engineering, JSCE,* 45 (A), March 1999, pp.1451-1459.

[7] Saidi, T., Furuuchi, H., and Ueda, T., "The transfer shear force-relative displacement relationship of the shear connector in steel-concrete sandwich beam and its model." *Doboku Gakkai Ronbunshuu E, JSCE*, Vol.64, No.1, February 2008, pp.122-141.

[8] Japanese Society of Civil Engineer., Standard specifications for hybrid structure, JSCE, December 2009. (in Japanese)

[9] Ros, S. and Shima, H., "New beam type test method for load-slip relationship of L-shape shear connector," *Proc. of 8th Symposium on Research and Application of Hybrid and Composite Structures, JSCE,* November 2009, Tokyo.

[10] Ros, S. and Shima, H., "Behaviors of L-shape shear connector subjected to strut compressive force in beam type test specimens." *Proceeding of the Japan Concrete Institute, JCI,* Vol.32, No.2, 2010, pp.1195-1200.

[11] Ros, S. and Shima, H., "Shear force-horizontal relative displacement relationship of L-shape shear connector subjected to strut compressive force in steel-concrete composite structures." *Doboku Gakkai Ronbunshuu A, JSCE,* Vol 66, No.4, 2010, pp.767-782.